

Design-related losses of double-fishnet negative-index photonic metamaterials

G. Dolling^{1*}, M. Wegener¹, C. M. Soukoulis^{2,3}, and S. Linden⁴

¹*Institut für Angewandte Physik and DFG-Center for Functional Nanostructures (CFN), Universität Karlsruhe (TH), Wolfgang-Gaede-Str. 1, D-76128 Karlsruhe, Germany*

²*Ames Laboratory and Department of Physics and Astronomy, Iowa State University, Ames, Iowa 50011, U.S.A.*

³*Institute of Electronic Structure and Laser at FORTH and Dept. of Materials Science and Technology, Univ. of Crete, Heraklion, Crete, Greece*

⁴*Institut für Nanotechnologie, Forschungszentrum Karlsruhe in der Helmholtz-Gemeinschaft, Postfach 3640, D-76021 Karlsruhe, Germany*

*Corresponding author: Gunnar.Dolling@physik.uni-karlsruhe.de

Abstract: The literature regarding the influence of the hole shape on the performance, especially on the losses, of negative-index metamaterials on the basis of the so-called double-fishnet structure is unclear. We investigate this aspect in a systematic theoretical study showing that the figure of merit can differ by as much as a factor of 2.5 between rectangular and circular holes, respectively.

© 2007 Optical Society of America

OCIS codes: (160.4760) Optical properties; (260.5740) Resonance; (999.9999) Metamaterials

References and links

1. V. M. Shalaev, "Optical negative-index metamaterials," *Nature Photon.* **1**, 41–48 (2006).
2. C. M. Soukoulis, S. Linden, and M. Wegener, "Negative Refractive Index at Optical Wavelengths," *Science* **315**, 47–49 (2007).
3. K. Busch, G. von Freymann, S. Linden, S. Mingaleev, L. Tkeshelashvili, and M. Wegener, "Periodic nanostructures for photonics," *Phys. Rep.* **444**, 101–202 (2007).
4. G. Dolling, C. Enkrich, M. Wegener, C. M. Soukoulis, and S. Linden, "Low-loss negative-index metamaterial at telecommunication wavelengths," *Opt. Lett.* **31**, 1800–1802 (2006).
5. G. Dolling, C. Enkrich, M. Wegener, C. M. Soukoulis, and S. Linden, "Simultaneous Negative Phase and Group Velocity of Light in a Metamaterial," *Science* **312**, 892–894 (2006).
6. G. Dolling, M. Wegener, C. M. Soukoulis, and S. Linden, "Negative-index metamaterial at 780 nm wavelength," *Opt. Lett.* **32**, 53–55 (2007).
7. U. K. Chettiar, A. V. Kildishev, H.-K. Yuan, W. Cai, S. Xiao, V. P. Drachev, and V. M. Shalaev, "Dual-Band Negative Index Metamaterial: Double-Negative at 813 nm and Single-Negative at 772 nm," *Opt. Lett.*, in press (2007).
8. Z. Ku and S. R. J. Brueck, "Comparison of negative refractive index materials with circular, elliptical and rectangular holes," *Opt. Express* **15**, 4515–4522 (2007).
9. G. Dolling, M. Wegener, and S. Linden, "Realization of a three-functional-layer negative-index photonic metamaterial," *Opt. Lett.* **32**, 551–553 (2007).
10. S. Zhang, W. Fan, K. J. Malloy, S. R. Brueck, N. C. Panou, and R. M. Osgood, "Near-infrared double negative metamaterials," *Opt. Express* **13**, 4922–4930 (2005).
11. J. B. Pendry, A. J. Holden, W. J. Stewart, and I. Youngs, "Extremely Low Frequency Plasmons in Metallic Mesostuctures," *Phys. Rev. Lett.* **76**, 4773 (1996).
12. G. Dolling, M. Wegener, A. Schädle, S. Burger, and S. Linden, "Observation of magnetization waves in negative-index photonic metamaterials," *Appl. Phys. Lett.* **89**, 231118 (2006).

1. Introduction

Negative-index photonic metamaterials operating at optical frequencies have recently attracted considerable attention because of novel opportunities in optics and photonics. Recent reviews can be found in Refs. [1–3]. One of the major challenges in this field lies in reducing the losses. It is clear that zero loss of the constitutive materials (dielectrics and metals) translates into zero loss of the metamaterial, provided that fabrication imperfections play no role. While the dielectric losses are indeed negligible at optical frequencies, the metal losses are considerable. (i) Thus, metal losses are one important aspect of the metamaterial loss. However, for a given metal and for a fixed operation wavelength, the metal losses are fixed. (ii) Yet, the metamaterial losses still depend on the metamaterial design, which determines the overlap of the light field and the lossy metal. Regarding aspect (i), it is now clear that silver-based structures exhibit a performance that is superior to that of gold-based structures. This claim stems from a direct comparison of experimentally and theoretically optimized structures for silver [3, 4] and gold [5] in the same wavelength regime. Moreover, the choice of silver (rather than gold) has been crucial for realizing negative-index metamaterials operating at the red end of the visible spectrum [6, 7]. In contrast, the literature regarding aspect (ii) is unclear for optical frequencies: While early work has suspected that rectangular shaped holes in double-layer fishnet structures are superior to circular holes [4, 5], a recent detailed study reported that the hole shape is not important at all [8] by comparing three particular gold-based samples with identical lattice constants.

The important question is whether this finding holds in general. As it is clearly relevant to search for low overall metamaterial loss, we choose silver rather than gold in the present study. Moreover, it is also clear that a meaningful comparison of different hole shapes requires a fixed operation wavelength in order to keep the metal losses constant.

2. Numerical calculations

The reference point for the present study is the standing record of a figure of merit $FOM \approx 3$ for a silver-based double-fishnet structure operating around $1.4\mu\text{m}$ wavelength [4]. The FOM is the negative ratio of real to imaginary part of the complex refractive index, i.e., $FOM = -\text{Re}(n)/\text{Im}(n)$. The details of this single-functional-layer structure – which has actually been fabricated and characterized interferometrically in detail – have been published [3, 4]. A corresponding three-functional-layer silver-based structure has delivered comparable performance [9]. Here, we search for an optimum circular-hole structure at the same operation wavelength as Ref. [4].

To follow the physics, it is helpful to briefly recall some known important aspects of the general design [10]: The double-fishnet structure can be viewed as composed of “magnetic atoms” and “electric atoms”. The electric atoms are just the long metal structures parallel to the incident electric-field vector. The resulting behavior is that of a diluted metal [11] with a plasma frequency which is lower than that of the bulk metal. Thus, these parts must be sufficiently wide (w_y in Fig. 1) to bring the effective plasma frequency slightly above the desired operation frequency, such that the real part of the effective electric permittivity is negative but not too large in magnitude. The resonance wavelength of the magnetic atoms is determined by the width w_x (see Fig. 1) of the structure. Intuitively, the magnetic-dipole moment stems from the anti-symmetric eigenmode of the two coupled metal layers, each of which can be viewed as a half-wavelength antenna (where “wavelength” refers to the effective local wavelength of the plasmonic excitation). Above the magnetic eigenfrequency, the magnetic susceptibility is negative and, hence, the magnetic permeability can be negative as well. In total, one has three free parameters for the rectangular-hole case: w_x , w_y , and the lattice constant a . In essence, the problem with circular holes is that one has just two rather than three free parameters, namely the

hole radius r and the lattice constant a . It would be purely coincidental if this reduced number of degrees of freedom delivered identical results. If, on the other hand, one acquires additional freedom by varying at least one further parameter, such as, e.g., the dielectric spacer thickness, one again has three free parameters and it appears possible in principle to achieve comparable performance with circular holes than with rectangular holes. However, these structures suffer from different problems to be discussed below.

To validate this qualitative overall reasoning, we proceed in two steps. (A) First, we fix the spacer thickness – as in Ref. [8] – and explicitly invalidate the general claim of Ref. [8] by example. (B) Second, we vary the spacer thickness at the same time.

For the numerical solutions of the three-dimensional vector Maxwell equations, we have previously employed (e.g., [12]) three different commercially available program packages that deliver consistent results: CST MicroWave Studio is a finite-difference time-domain approach, Comsol Multiphysics is a finite-element frequency-domain approach, and JCMSuite is also a finite-element frequency-domain approach. The results actually shown in this article have been obtained by CST MicroWave Studio.

The optical parameters of silver and the MgF₂ dielectric spacer are chosen as previously [4]. In brief, we use the free-electron Drude model with plasma frequency $\omega_{\text{pl}} = 1.37 \cdot 10^{16} \text{ s}^{-1}$ and collision frequency $\omega_{\text{col}} = 8.5 \cdot 10^{13} \text{ s}^{-1}$ for silver. The MgF₂ refractive index is taken as $n = 1.38$. Following our Ref. [4], we embed the double-fishnet structure in an effective homogeneous medium with a refractive index of $n = \sqrt{1.1}$, whereas the structures are usually located on a glass substrate in experiments. This simplification is unproblematic unless Wood anomalies arising from diffraction of light into the substrate spectrally merge with the metamaterial resonances. Obviously, one is leaving the effective-medium limit in this case, which implies that a description in terms of effective material parameters becomes meaningless. This aspect will become relevant in step (B) below but is unimportant for step (A).

(A) We start from the vertical layer thicknesses Ag ($t = 45 \text{ nm}$), MgF₂ ($s = 30 \text{ nm}$), and Ag ($t = 45 \text{ nm}$) that have been reported in Ref. [4]. Lateral parameters have been $w_x = 316 \text{ nm}$, $w_y = 100 \text{ nm}$, and $a = 600 \text{ nm}$. The resulting FOM ≈ 3 is the best experimentally verified value available at present (see Fig. 1(a)). We emphasize that this is not even the best theoretically possible set of parameters for rectangular holes. For example, for $t = 45 \text{ nm}$, $s = 30 \text{ nm}$, $w_x = 351 \text{ nm}$, $w_y = 100 \text{ nm}$, and $a = 500 \text{ nm}$ we find a FOM = 3.72 at around $1.4 \mu\text{m}$ wavelength.

To find the best theoretically possible values for square-shaped holes, we proceed as follows. We simultaneously vary a and $w = w_x = w_y$ and keep the operation wavelength fixed at $1.4 \mu\text{m}$ and search for an optimum of the FOM at this wavelength. For circular holes, we proceed analogously by varying a and r . The effective-parameter retrieval underlying the determination of the FOM has been described in detail in Ref. [4]. The results of these optimizations are depicted in Figs. 1 (b) and (c), revealing an optimum FOM of 1.29 and 1.21 for square-shaped and circular holes, respectively. While the resulting FOM for square-shaped and circular holes are quite similar, they both differ by about a factor of 2.5 from the FOM for the rectangular-hole case. These larger losses for the square/circular holes mainly originate from a deteriorated magnetic resonance that barely shows a negative real part of the magnetic permeability above resonance. This means that these samples are not really double negative [1]. The real part of the electric permittivity of the square/circular holes is even more negative than in the rectangular-hole case due to the larger volume fraction of metal in the diluted-metal parts. This overall behavior supports our above qualitative reasoning in that one generally does not have a sufficient number of free parameters for the loss optimization in the square/circular-hole case.

To further test this qualitative reasoning, we have performed additional calculations for elliptical holes. We search for an optimum FOM for a fixed operation wavelength of $1.4 \mu\text{m}$, by simultaneously varying the *three* free parameters r_x (short axis of the ellipse), r_y (long axis of

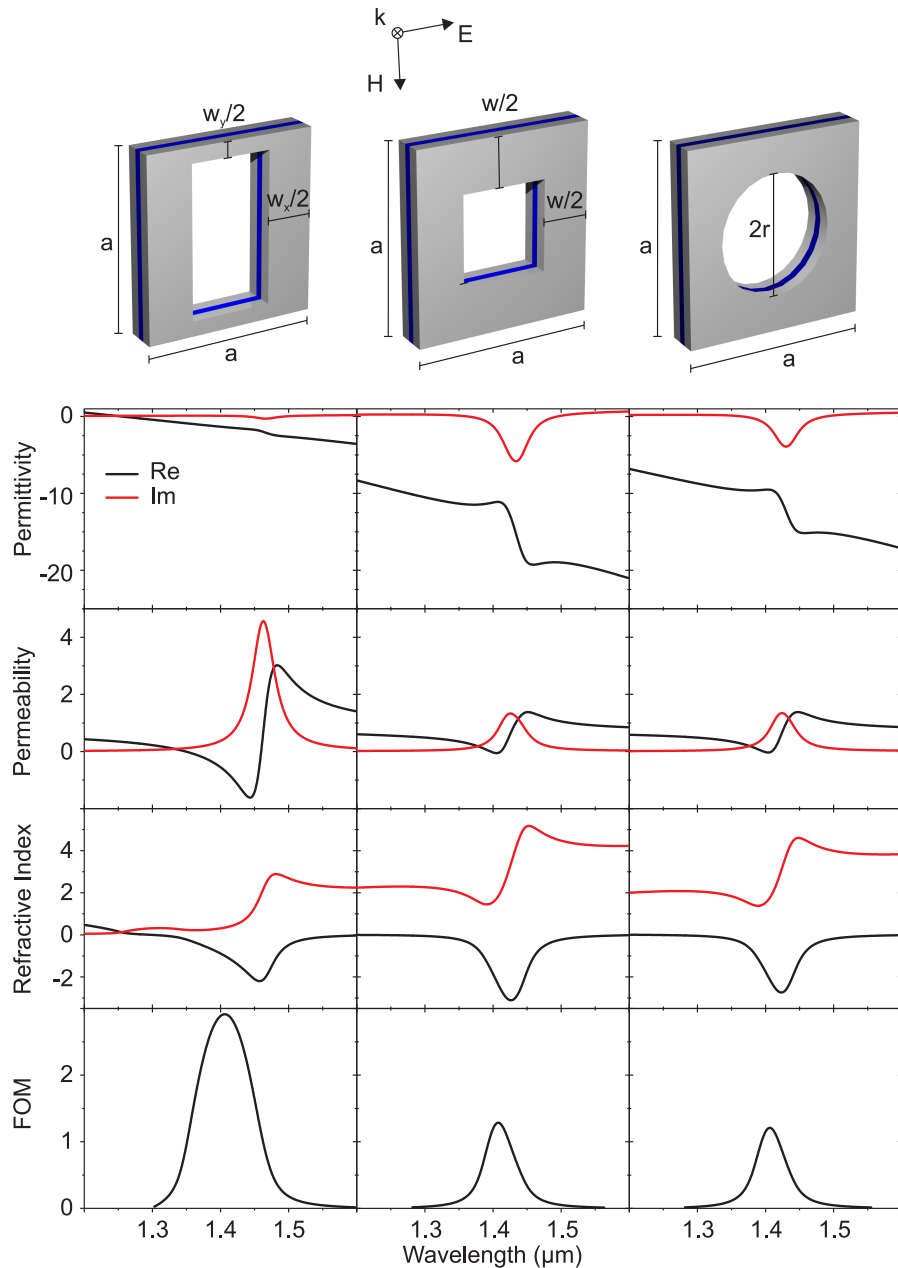


Fig. 1. Comparison of rectangular, square, and circular-shaped holes in double-layer fishnet structures. The three columns represent the three hole shapes, which are indicated on the top. The polarization configuration is also shown on the top. The rows below show the real and imaginary parts of the retrieved effective electric permittivity ϵ , the magnetic permeability μ , the refractive index n , and the resulting figure of merit $FOM = -\text{Re}(n)/\text{Im}(n)$. The parameters for rectangular holes $w_x = 316\text{nm}$, $w_y = 100\text{nm}$, and $a = 600\text{nm}$ correspond to those of Ref. [4]. The best parameters that we have found here for square-shaped holes are $w_x = w_y = w = 319\text{nm}$ and $a = 625\text{nm}$; for circular holes $r = 192\text{nm}$ and $a = 625\text{nm}$. The vertical layer thicknesses are kept fixed for all three hole shapes: 45 nm Ag (gray), 30 nm MgF_2 (blue), and 45 nm Ag (gray).

Table 1. FOM of circular-hole double-fishnet negative-index photonic metamaterials obtained by embedding the structure in an effective homogeneous medium with refractive index $n = \sqrt{1.1}$ (i.e., no glass substrate). The FOM values in brackets refer the corresponding calculations for structures in air ($n = 1$) on a glass substrate with refractive index $n = 1.5$. The thickness of the spacer layer increases from $s = 30$ nm in the top to $s = 100$ nm in the bottom row. The metal thickness $t = 45$ nm is fixed. To keep a fixed vacuum wavelength $\lambda = 1.4 \mu\text{m}$, the lattice constant a , and the hole radius r have to be adjusted. The column labeled λ/a refers to the ratio of vacuum wavelength and lattice constant. The column to the right refers to the corresponding ratio for the material wavelength (λ/n) in the embedding medium with refractive index $n = \sqrt{1.1}$ (glass substrate with refractive index $n = 1.5$).

s	a	r	λ	λ/a	$(\lambda/n)/a$	FOM
30 nm	625 nm	192 nm	$1.406 \mu\text{m}$	2.25	2.15 (1.50)	1.21 (0.99)
40 nm	670 nm	191 nm	$1.407 \mu\text{m}$	2.10	2.00 (1.40)	1.47 (1.09)
50 nm	700 nm	188 nm	$1.404 \mu\text{m}$	2.01	1.91 (1.34)	1.78 (1.35)
60 nm	735 nm	201 nm	$1.406 \mu\text{m}$	1.91	1.82 (1.28)	2.11 (1.31)
70 nm	755 nm	197 nm	$1.409 \mu\text{m}$	1.87	1.78 (1.24)	2.41 (1.48)
80 nm	780 nm	211 nm	$1.409 \mu\text{m}$	1.81	1.72 (1.20)	2.74 (1.35)
90 nm	800 nm	221 nm	$1.410 \mu\text{m}$	1.76	1.68 (1.18)	3.06 (1.15)
100 nm	820 nm	241 nm	$1.405 \mu\text{m}$	1.71	1.63 (1.14)	3.37 (0.88)

the ellipse), and a . For $r_x = r_y = r$, circular holes are recovered. The other parameters are chosen identical to those of Fig. 1. Under these conditions, we find an optimum of $\text{FOM} = 3.16$ at $1.405 \mu\text{m}$ wavelength for $r_x = 123$ nm, $r_y = 223$ nm, and $a = 535$ nm. This FOM is comparable to that of the rectangular holes and again considerably larger than that for circular/square holes, in agreement with our qualitative reasoning.

(B) Next, we vary the thickness s of the dielectric MgF_2 spacer layer. We start by continuing along the lines of (A) in that we consider a metamaterial embedded in an effective dielectric environment, i.e., we do not account for a substrate. Again, the operation wavelength is fixed to $\lambda = 1.4 \mu\text{m}$ to allow for direct comparison with the above rectangular-hole structures. The small variations of λ in Table 1 are due to limited computation time.

As the spacer thickness s is increased from 30 nm to 100 nm in Table 1, a and r have to be increased to keep the vacuum wavelength λ fixed. The FOM increases from 1.21 to 3.37 which seemingly outperforms the optimum rectangular holes. Even without a glass substrate, however, several parameter choices exhibit values $(\lambda/n)/a < 2$, where $n = \sqrt{1.1}$ is the refractive index of the embedding medium. Recall that the ratio $(\lambda/n)/a = 2$ corresponds to the fundamental Bragg condition. Hence, for ratios below 2, the effective-medium approximation can be questionable.

The situation becomes even worse if the glass substrate is accounted for. To further investigate this aspect, we have repeated the calculations for the double-fishnet structure in air located on a glass substrate. The corresponding FOM values are given in brackets in Table 1. Obviously, they are generally lower. Moreover, the FOM first increases with increasing s but then drops again, reaching a maximum value of $\text{FOM} = 1.48$ for the circular holes at $s = 70$ nm. The reason underlying this drastic influence of the substrate is the Wood anomaly corresponding to diffraction of light into the substrate (i.e., $(\lambda/n)/a = 1$ with the glass-substrate refractive index $n = 1.5$) that gradually shifts towards the magnetic resonance with increasing s , hence increasing a , and eventually overlaps with it. This overlap deteriorates the metamaterial performance, especially its FOM. Moreover, an interpretation of the results in terms of an effective material is highly questionable at this point as $1 \approx (\lambda/n)/a < 2$.

The bottom line of part (B) is that the FOM of the circular holes can only be increased slightly by varying the dielectric-spacer thickness.

3. Conclusions

In conclusion, the so-called double-fishnet structure is presently the most promising design for negative-index metamaterials operating at optical frequencies. We have presented a systematic theoretical study on the influence of the hole shape on the metamaterial losses. For fixed vertical layer sequence and fixed operation wavelength, the hole shape has a large influence on the losses. Clearly, this finding does not exclude the possibility of special operation frequencies for which the hole shape accidentally has no large influence. Indeed, as the operation frequency increases towards the red end of the visible, the rectangular holes tend to become more square-shaped, and the difference between rectangular/square/elliptical/circular holes becomes quite small.

Acknowledgments

We acknowledge support by the Deutsche Forschungsgemeinschaft (DFG) and the State of Baden-Württemberg through the DFG-Center for Functional Nanostructures (CFN) within sub-project A1.5. The research of S. L. is further supported through a “Helmholtz-Hochschul-Nachwuchsgruppe” (VH-NG-232). Work at the Ames Laboratory was supported by the Department of Energy (Basic Energy Sciences) under Contract No. DE-AC02-07CH11358. This work was partially supported by the AFOSR under MURI grant (FA9550-06-1-0337), by Department of the Navy, Office of Naval Research (Award No. N00014-07-1-0359), and EU FET projects Metamorphose and PHOREMOST. The PhD education of G. D. is further supported by the Karlsruhe School of Optics & Photonics (KSOP).